

Many-Body Localization and Particle Statistics in Disordered Bose-Hubbard Model

Jie Chen,^{1,2,*} Chun Chen,^{1,†} and Xiaoqun Wang^{3,4,‡}

¹Key Laboratory of Artificial Structures and Quantum Control (Ministry of Education),
School of Physics and Astronomy, Shanghai Jiao Tong University, Shanghai 200240, China

²School of Science, Key Laboratory of High Performance Scientific Computation, Xihua University, Chengdu 610039, China

³School of Physics, Zhejiang University, Hangzhou 310058, Zhejiang, China

⁴Collaborative Innovation Center of Advanced Microstructures, Nanjing University, Nanjing 210093, China

We study the potential influence of the particle statistics on the stability of the many-body localization in the disordered Bose-Hubbard model. Within the higher-energy section of the dynamical phase diagram, we find that there is no apparent finite-size boundary drift between the thermal phase and the many-body localized regime. We substantiate this observation by introducing the Van Vleck perturbation theory into the field of many-body localization. The appropriateness of this method rests largely on the peculiar Hilbert-space structure enabled by the particles' Bose statistics. The situation is reversed in the lower-energy section of the dynamical phase diagram, where the significant finite-size boundary drift pushes the putative many-body localized regime up to the greater disorder strengths. We utilize the algebraic projection method to make a connection linking the disordered Bose-Hubbard model in the lower-energy section to an intricate disordered spin chain model. This issue of the finite-size drift could hence be analogous to what happens in the disordered Heisenberg chain. Both trends might be traced back to the particles' intrinsic or emergent Fermi statistics.

Introduction. The current research on many-body localization (MBL) is severely hindered by the finite-size drift of the boundary between the thermal phase and the putative MBL regime [1–7]. This kind of drift arises in plenty of theoretical models including the disordered Heisenberg spin chain [8–10], literally plaguing most numerical studies in the field and impeding our understanding of the MBL phenomenon.

In this regard, search for a new model system without this issue could be instrumental in the broader research endeavor to pursue the nonergodic eigenstate matter. As advocated by the present work, the disordered Bose-Hubbard (dBH) model [11–14] realizable in cold-atom labs [15, 16] might provide such a candidate system. Concretely, stimulated by the question concerning the relationship between MBL and particle statistics in general and the clustering of interacting bosons in random potentials in particular, we identify the robust and peculiar localization signature that is suggestive of the existence of a novel cluster MBL regime in the higher-energy section of the dBH model's dynamical phase diagram. Our results hint that it is not very likely for the dBH chain to fully thermalize even at weak disorder when the energy density is high [17]. The claimed cluster MBL regime can thus avoid the problem of finite-size drift and persist still in the thermodynamic limit.

To facilitate the investigation, new methods are proposed. On the higher-energy side, we first introduce the Van Vleck perturbation theory [18–20] into the study of MBL, which exploits the formation of well-separated eigenstate manifolds and the damped hybridizing between the slow intra- and fast inter-manifold degrees of freedom given the clustering endowed by particles' Bose statistics. On the lower-energy side, we next use the algebraic projection method [21, 22] to expose the resembling between the dBH model and a disordered spin chain, where the emergent Fermi statistics plays a key role.

Model. The periodic dBH Hamiltonian is described by

$$H_{\text{dBH}} = -J \sum_{i=1}^L (a_i^\dagger a_{i+1} + \text{H.c.}) + \sum_{i=1}^L \frac{U}{2} n_i (n_i - 1) + \sum_{i=1}^L \mu_i n_i \quad (1)$$

where a_i^\dagger (a_i) is the boson creation (annihilation) operator at site i , $n_i = a_i^\dagger a_i$ ($N = \sum_i^L n_i$) counts the local (total) boson occupation number, U parametrizes the onsite Hubbard repulsion, and $\mu_i \in [-\mu, \mu]$ is a diagonal random potential drawn from the box distribution. Crucially, $[N, H_{\text{dBH}}] = 0$, so the number-conserving dBH model respects the $U(1)$ symmetry. In this work, all relevant quantities are averages over a sufficient amount of random samples, solved by exact diagonalization (ED) [23] or the Van Vleck perturbative method [18]. We set $J = 1$ as the energy unit and fix $U = 3J$, $N = \frac{L}{2}$ in the subsequent numeric calculations.

Absence of drift in finite-size scaling of level-spacing ratio and maximal site occupation. It is critical practice to examine how the various phase-regime boundaries of the dynamical phase diagram of the dBH model change under the increase of system size. To this aim, we conduct extensive numerical calculations to construct the finite-size dynamical phase diagrams of the dBH chain from $L = 8$ up to $L = 14$. Figures 1 and 2 illustrate the obtained ED results based respectively on level-spacing ratio [12, 24, 25] and maximal site occupation.

There are two messages from Fig. 1. First, there is a pronounced drift of the boundary between the thermal phase and the MBL regime in the lower-energy section of the dynamical phase diagram. Such a drift under the increase of L toward greater disorder strengths echoes what occurs in the disordered Heisenberg chain and is known to be the obstacle toward identifying MBL as a phase of matter. Secondly, the MBL regime in the higher-energy section of the dynamical phase diagram appears robust and stable. Especially, the boundary between the cluster MBL regime and the thermal phase is moving downward to the spectrum center $\varepsilon \approx 0.5$, suggesting the absence of drift and the persistence of both this MBL regime and the mobility edge in the large-size limit. Recall that the density of states across the higher-energy section is enhanced upon this successive increase of μ [26]. Finally, Fig. 2 shows that the two messages from Fig. 1 can also be

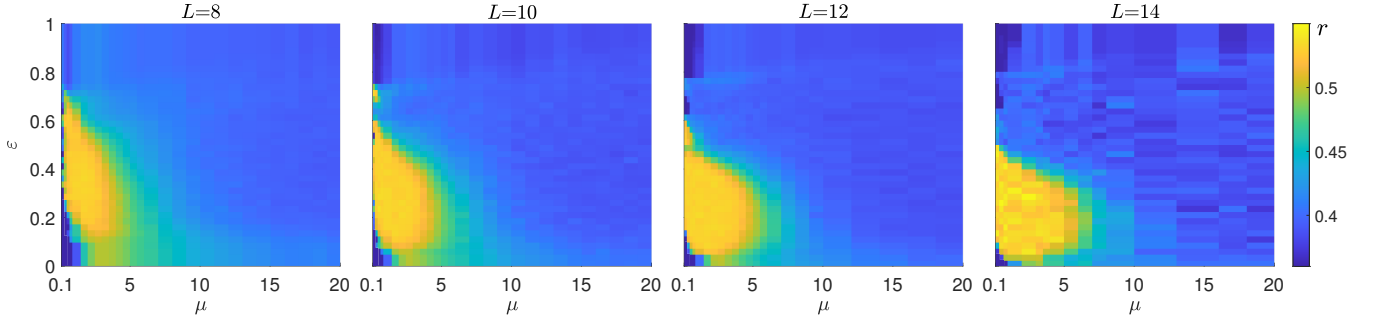


FIG. 1. The sequence of small-size dynamical phase diagrams of the dBH chain with $N = \frac{L}{2}$. The color contours are derived from the level-spacing ratio r computed by ED and averaged over many random samples. ε and μ stand for the energy density and the disorder strength.

probed via the more accessible quantity, the maximal site occupation $\max(n_i)/N$, thereby being experimentally testable.

Hereafter, our strategy is to gain an overall understanding of the dynamical phase diagram of the dBH model by exploring the distinction in the emergent particle statistics from the opposite higher- and lower-energy limits of the phase diagram.

Higher-energy limit: confirming absence of drift via the Van Vleck perturbation theory. As per (1), one can divide H_{dBH} into two categories: the off-diagonal $H_J = -J \sum_{i=1}^L (a_i^\dagger a_{i+1} + \text{H.c.})$ and the diagonal $H_U = \sum_{i=1}^L \frac{U}{2} n_i (n_i - 1)$ and $H_\mu = \sum_{i=1}^L \mu_i n_i$. As H_J is a single-particle hopping term, in the higher-energy limit, the skeleton of the H_{dBH} matrix is built upon the H_U term, which itself is structured into the individual diagonal blocks upon the basis states shared the same maximal onsite boson occupation number $n_{\text{max}} = 1, \dots, \frac{L}{2}$. H_μ respects this diagonal block structure. In addition, while H_J creates off-diagonal matrix elements within each n_{max} block, it also engenders off-diagonal matrix elements connecting the n_{max} block to its two neighbor blocks $n_{\text{max}} \pm 1$, thus furnishing a nice block-tridiagonal structure. When $n_{\text{max}} = 1, \frac{L}{2}$, there is one such neighboring block. To some extent, n_{max} may be regarded as an approximate quantum number once these off-diagonal inter-block submatrices are removed. As shown below, the Van Vleck perturbation theory [18–20] serves exactly this task.

To proceed, let us temporarily neglect H_J and make a comparison between the portions of the $H_U + H_\mu$ matrix within the lower- and higher-energy sections of the phase diagram, assuming μ is small and any accidental symmetry is broken.

This diagonal $H_U + H_\mu$ matrix can be arranged into $\frac{L}{2}$ blocks according to n_{max} . Each eigenstate now is simply specified by the $\{n_i\}$ set; it hence represents trivially the local integrals of motion (LIOMs) [27–30]. For large- n_{max} blocks, bosons of these LIOMs are more concentrated on several local sites, but for small- n_{max} blocks, they spread more uniformly across the whole chain. In the absence of both H_J and H_μ , the bottom $n_{\text{max}} = 1$ block is flat and there is a gap U separating it from the $n_{\text{max}} = 2$ block. This gap increases linearly with n_{max} . But, as the energy range of the $n_{\text{max}} = 2$ block is extensive, there is a substantial energy overlap between the $n_{\text{max}} = 2$ and 3 blocks. Such a trend continues in the lower-energy section of the phase diagram. In contrast, near the top $n_{\text{max}} = \frac{L}{2}$ block, the situation alters sharply. Due to Bose statistics, n_{max} in this circumstance can be huge such that the large- n_{max} blocks comprising the higher-energy section of the phase diagram are well separated in energy scale even for moderate U : they form distinguishing manifolds without energy overlaps.

The Van Vleck approximation is to devise a suitable canonical transformation e^{iS} to perturbatively achieve the goal that the transformed Hamiltonian $H'_{\text{dBH}} = e^{iS} H_{\text{dBH}} e^{-iS}$ preserves the same eigenenergies with the same degeneracy as the original Hamiltonian H_{dBH} but simultaneously has no matrix elements between the unperturbed blocks up to the desired order of the small perturbation. Focus on the higher-energy section of the phase diagram, one can choose the unperturbed Hamiltonian $H^0 = H_U + H_\mu$ and the small perturbation $JV = H_J$. By demanding the canonical transformation $S = S^\dagger$ to be fully off-block-diagonal, i.e., $\langle i, \alpha | S | j, \alpha \rangle = 0$ (see definitions below), one can explicitly construct, up to third order of JV , the transformed block diagonal Hamiltonian as follows,

$$\begin{aligned}
\langle i, \alpha | H'_{\text{dBH}} | j, \alpha \rangle &= E_{i\alpha}^0 \delta_{ij} + \langle i, \alpha | JV | j, \alpha \rangle + \frac{1}{2} \sum_{k, \gamma \neq \alpha} \langle i, \alpha | JV | k, \gamma \rangle \langle k, \gamma | JV | j, \alpha \rangle \left(\frac{1}{E_{i\alpha}^0 - E_{k\gamma}^0} + \frac{1}{E_{j\alpha}^0 - E_{k\gamma}^0} \right) \\
&+ \frac{1}{2} \sum_{l, \eta \neq \alpha} \left\{ \sum_{k, \gamma \neq \alpha} \left[\frac{\langle i, \alpha | JV | k, \gamma \rangle \langle k, \gamma | JV | l, \eta \rangle \langle l, \eta | JV | j, \alpha \rangle}{(E_{i\alpha}^0 - E_{k\gamma}^0)(E_{i\alpha}^0 - E_{l\eta}^0)} + \frac{\langle i, \alpha | JV | l, \eta \rangle \langle l, \eta | JV | k, \gamma \rangle \langle k, \gamma | JV | j, \alpha \rangle}{(E_{j\alpha}^0 - E_{k\gamma}^0)(E_{j\alpha}^0 - E_{l\eta}^0)} \right] \right\} \\
&- \frac{1}{2} \sum_{l, \eta \neq \alpha} \left\{ \sum_{k, \gamma \neq \eta} \left[\frac{\langle i, \alpha | JV | k, \gamma \rangle \langle k, \gamma | JV | l, \eta \rangle \langle l, \eta | JV | j, \alpha \rangle}{(E_{i\alpha}^0 - E_{l\eta}^0)(E_{k\gamma}^0 - E_{l\eta}^0)} + \frac{\langle i, \alpha | JV | l, \eta \rangle \langle l, \eta | JV | k, \gamma \rangle \langle k, \gamma | JV | j, \alpha \rangle}{(E_{j\alpha}^0 - E_{l\eta}^0)(E_{k\gamma}^0 - E_{l\eta}^0)} \right] \right\} + \dots \quad (2)
\end{aligned}$$

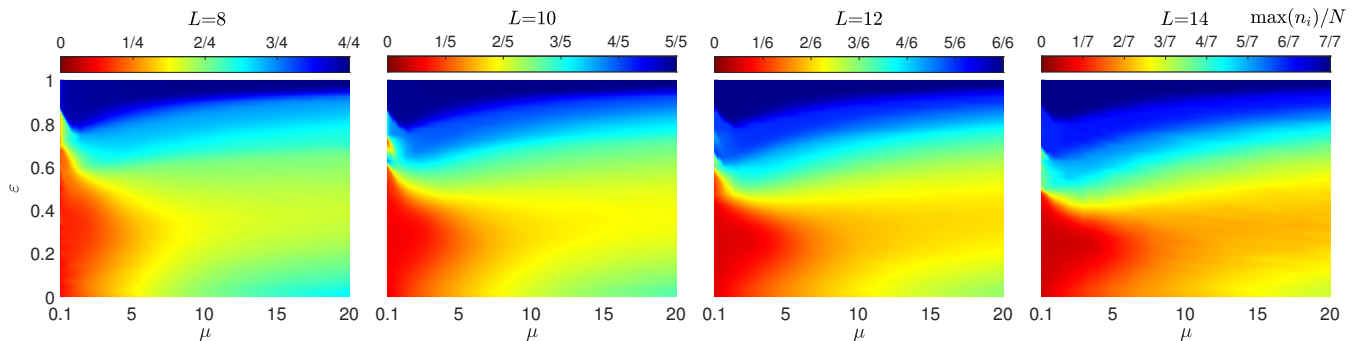


FIG. 2. The sequence of small-size dynamical phase diagrams of the dBH chain with $N = \frac{L}{2}$. The color contours are drawn from the maximal site occupation $\max(n_i)/N$ computed via ED and averaged over many random realizations.

Here α, γ, η are the unperturbed block- n_{\max} indices. For a particular block, the involved ket and bra vectors indexed by i, j, k, l are its corresponding eigenstates of the unperturbed H^0 , i.e., $H^0|i, \alpha\rangle = E_{i\alpha}^0|i, \alpha\rangle$. Once H'_{dBH} is available for block α , one can exact diagonalize the resulting matrix (2) to get the perturbative estimates of the eigenenergies of H_{dBH} with respect to this emergent quantum number n_{\max} . It is crucial that while the inter-block off-diagonal matrix elements are only eliminated perturbatively, the intra-block off-diagonal matrix elements are treated almost exactly. The obtained eigenfunctions of H'_{dBH} would typically have degraded accuracy, so they were seldom used to extract the wavefunction-related information, such as the entanglement entropy.

For large- n_{\max} blocks in the higher-energy section of the phase diagram, both the large intra-block H_U values and the ensuring large inter-block energy gaps guarantee the comparative smallness of the perturbation H_J , which, in turn, renders the outlined computational scheme founded upon the Van Vleck degenerate perturbation theory particularly appealing in helping understand the cluster MBL regime at weak disorder.

In view of the importance of both the identification of n_{\max} and the perturbativeness of H_J in setting up the algorithm, it is intriguing that the self-consistency and the applicability of the celebrated Van Vleck perturbation theory to the dBH type model are essentially enabled by the particles' Bose statistics.

Potentially, the proposed Van Vleck algorithm could have practical and theoretical significance. On the practical side, the Hilbert-space size of the half-filled dBH chain grows rapidly with the chain length as $\frac{(3L/2-1)!}{(L/2)!(L-1)!}$. While, for $L = 14$, this size is 77520, it jumps to 490314 for $L = 16$ and 3124550 for $L = 18$. Considering the needs of random averages, this means that even for shift-invert or polynomially filtered methods, it is impractical to perform an exact scaling analysis of the pertinent quantities covering longer bosonic chains. In this regard, the Van Vleck algorithm may provide an alternative to partly tackle this problem. We explicitly test this possibility in Fig. 3 where we restrict attention to the three largest- n_{\max} blocks, $N, N-1$, and $N-2$, and succeed in ex-

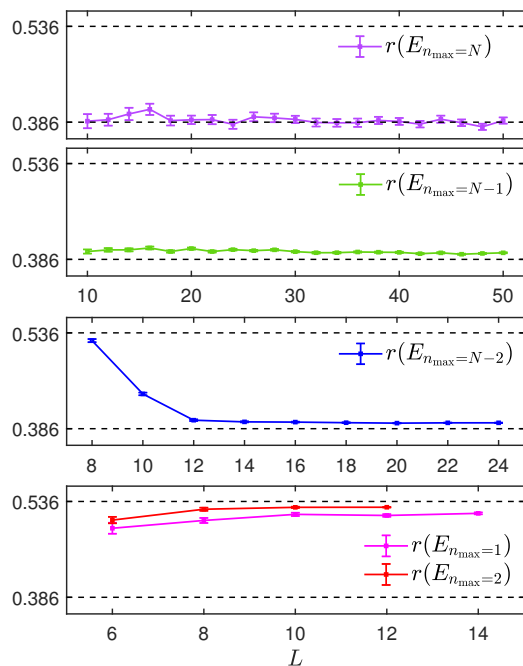


FIG. 3. Perturbative estimates of the level-spacing ratio r for the top blocks $n_{\max} = N, N-1, N-2$ and bottom blocks $n_{\max} = 1, 2$ as a function of the dBH chain length L . These scaling results are obtained by the Van Vleck algorithm and averaged over at least 100 random samples at weak disorder $\mu = 2J$.

cutting the Van Vleck algorithm to manifest, especially from small to medium lengths, the persistent convergence of the averaged level-spacing ratio r toward Poisson in a weak-disorder BH chain up to $L = 50$ for blocks $N, N-1$ and up to $L = 24$ for block $N-2$. Particularly, a clean crossover of r from GOE to Poisson is revealed in block $N-2$ upon raising L . Therefore, in accord with the exact scaling trend perceived from the small chains (Figs. 1 and 2), on the theoretical side, the scaling analysis based on these perturbative long-chain results (Fig. 3) tentatively confirms our key speculations on the sta-

bilization of the cluster MBL regime and, more importantly, the absence of finite-size drift in the higher-energy section of the phase diagram. For completeness, we also extend the Van Vleck method to the bottom of the phase diagram and consistently recover the convergent trend of r toward GOE in the lowest two blocks $n_{\max} = 1$ and 2, verifying the applicability of the method to a wider parameter space. Admittedly, it is worth cautioning that, unlike the top and bottom blocks, for those decisive n_{\max} in the middle of the spectrum, both the block size and the complexity of (2) get enhanced enormously such that the Van Vleck algorithm again becomes impractical.

Lower-energy limit: mapping to disordered spin chain via algebraic projection method. Contrastingly, due to the energy penalty from the onsite Hubbard repulsion, the lower-energy eigenstates of (1) comprise the state configurations featuring low local boson concentrations.

To uncover the emergent spin/fermion degrees of freedom in this bosonic model [21, 22, 31], we illustrate here that the lower-energy portion of the dBH model's dynamical phase diagram (Fig. 1) can be qualitatively understood by connecting it to the disordered spin chain using the algebraic projection method. To this end, we introduce the projector \mathcal{P} that projects onto the subspace \mathcal{C} subtended by an ensemble of eigenvectors satisfying the hard-core constraint meaning that the onsite boson occupation number on any lattice site is no more than 1. Likewise, the complement projector \mathcal{Q} that projects onto the supplementary Hilbert space is defined by $\mathcal{Q} = 1 - \mathcal{P}$. Strictly speaking, within \mathcal{C} , the Hubbard U term has no contribution. Therefore, unlike the study of equilibrium ground-state physics, in the algebraic projection approach, the perturbative treatment of the virtual hopping processes [see (7) below] is due to the imposition of projectors \mathcal{P} and \mathcal{Q} irrespective of the values of U and J . Symbolically, the dBH Hamiltonian can now be written as a matrix, $\begin{bmatrix} \mathcal{P}H_{\text{dBH}}\mathcal{P} & \mathcal{P}H_{\text{dBH}}\mathcal{Q} \\ \mathcal{Q}H_{\text{dBH}}\mathcal{P} & \mathcal{Q}H_{\text{dBH}}\mathcal{Q} \end{bmatrix}$. Our intent is to derive an

effective Hamiltonian H_{eff} capturing perturbatively the influence of $\mathcal{Q}H_{\text{dBH}}\mathcal{Q}$ onto $\mathcal{P}H_{\text{dBH}}\mathcal{P}$ via the two off-diagonal couplings $\mathcal{P}H_{\text{dBH}}\mathcal{Q}$ and $\mathcal{Q}H_{\text{dBH}}\mathcal{P}$. Operationally, such physical processes are encapsulated in the procedure of an approximate block diagonalization of the above matrix. Recall that for a usual 2×2 matrix $\begin{bmatrix} a & b \\ c & d \end{bmatrix}$, its two eigenvalues are $\frac{1}{2}(a + d \mp \sqrt{(a - d)^2 + 4bc})$. Then, under the assumption that the operator norm $\|\mathcal{P}H_{\text{dBH}}\mathcal{P}\| \ll \|\mathcal{Q}H_{\text{dBH}}\mathcal{Q}\|$, it is easy to derive that

$$H_{\text{eff}} \approx \mathcal{P}H_{\text{dBH}}\mathcal{P} - \mathcal{P}H_{\text{dBH}}\mathcal{Q} \frac{1}{\mathcal{Q}H_{\text{dBH}}\mathcal{Q}} \mathcal{Q}H_{\text{dBH}}\mathcal{P}, \quad (3)$$

where we omit the higher-order corrections [32]. Alternatively, using resolvent [19], one can show that

$$[\mathcal{P}H_{\text{dBH}}\mathcal{P} - \mathcal{P}H_{\text{dBH}}\mathcal{Q} \frac{1}{\mathcal{Q}H_{\text{dBH}}\mathcal{Q}} \mathcal{Q}H_{\text{dBH}}\mathcal{P}][\mathcal{P} \frac{1}{H_{\text{dBH}}} \mathcal{P}] = 1. \quad (4)$$

This instead is an exact identity.

Let us begin with the first term of H_{eff} . As usual, the effect of \mathcal{P} can be realized by imposing the hard-core boson constraint, which, in terms of spin- $\frac{1}{2}$ Pauli matrices, can be expressed as the following mapping,

$$a_i \rightarrow \sigma_i^+, \quad a_i^\dagger \rightarrow \sigma_i^-, \quad 1 - 2n_i \rightarrow \sigma_i^z. \quad (5)$$

Thus, under the hard-core boson limit,

$$\mathcal{P}H_{\text{dBH}}\mathcal{P} = -\frac{J}{2} \sum_{i=1}^L (\sigma_i^x \sigma_{i+1}^x + \sigma_i^y \sigma_{i+1}^y) + \sum_{i=1}^L \frac{\mu_i}{2} (1 - \sigma_i^z). \quad (6)$$

It is ready to recognize that $\mathcal{P}H_{\text{dBH}}\mathcal{P}$ is a disordered XX spin chain, which is Anderson localized in 1D. Meanwhile, upon increasing U to infinity, $\mathcal{P}H_{\text{dBH}}\mathcal{P}$ would be the only remaining term in H_{dBH} and the dBH model in this limit becomes a free-fermion chain. In this sense, the genuine many-body interaction effects in H_{eff} shall arise for moderate U and they stem mainly from the second as well as those omitted higher-order correction terms in (3).

Next, for the second term of H_{eff} , we would only consider the second-order virtual hopping processes, yielding

$$\begin{aligned} & -\mathcal{P}H_{\text{dBH}}\mathcal{Q} \frac{1}{\mathcal{Q}H_{\text{dBH}}\mathcal{Q}} \mathcal{Q}H_{\text{dBH}}\mathcal{P} \\ & \approx -J^2 \sum_{i=1}^L \mathcal{P}(a_{i-1}^\dagger + a_{i+1}^\dagger) a_i \frac{n_i - 1}{U + \sum_{j=1}^L \mu_j n_j} a_i^\dagger (a_{i-1} + a_{i+1}) \mathcal{P} \\ & \approx \sum_{i=1}^L (\sigma_{i-1}^- + \sigma_{i+1}^-) \sigma_{i+1}^+ \frac{(-4J^2)}{2U + 4\mu_i + \sum_{j \neq i, i+1} \mu_j (1 - \sigma_j^z)} \\ & + \sum_{i=1}^L (\sigma_{i-1}^- + \sigma_{i+1}^-) \sigma_{i-1}^+ \frac{(-4J^2)}{2U + 4\mu_i + \sum_{j \neq i, i-1} \mu_j (1 - \sigma_j^z)}, \quad (7) \end{aligned}$$

where in middle steps we replace \mathcal{Q} by the equivalent operator $n_i - 1$ and then \mathcal{P} is removed after invoking (5).

Collectively, up to second-order perturbation, the effective spin Hamiltonian H_{eff} capable of qualitatively describing the lower-energy portion of the dynamical phase diagram of the dBH model is given by summing up (6) and (7). For the case $\mu_i = 0$, this result was obtained before by [21]. However, it is interesting that when $\mu_i \neq 0$ and under the lower-energy limit, besides the resulting diagonal disordered σ^z -fields in the noninteracting part of H_{eff} , i.e., (6), the leading off-diagonal many-body interacting part of H_{eff} , i.e., (7), becomes randomized as well, whose disorder strength is further characterized by a dynamical dependence on the particular σ^z -configuration of the acted basis state.

As (6) is Anderson localized, the significant finite-size drift seen in Figs. 1 and 2 at $U = 3J$ that obscures the identification of MBL in dBH chain shall originate from the revealed longer-range multi-spin interactions in (7). In light of the importance of the dBH model in experiments [15, 16], the derived disordered interacting spin model (7) may itself be an intriguing model for the future study of MBL in bosonic systems.

In essence, the above analysis indicates that the lower-energy nonequilibrium physics of the dBH model is largely governed by the particles' emergent spin or Fermi statistics.

Conclusion. Like dimension and symmetry, particle statistics can influence the eigenstate matter formation. Through the introduction of the Van Vleck perturbation theory tailored for handling the clustering structures due to Bose statistics, we are tempted to speculate on the absence of the finite-size

drift and the robustness of the cluster MBL regime in the higher-energy section of the dBH model's dynamical phase diagram. Next, via the algebraic projection approach, the persisting finite-size drift and the successive enlargement of the thermal phase in the lower-energy section of the same phase diagram are then partially explained by invoking the emergent Fermi statistics to map this bosonic model onto a disordered spin chain. These disparate scaling behaviors hint that the Bose-Fermi distinction in the particle statistics may delineate a mobility edge in between the cluster MBL regime in the higher-energy section and the thermal phase in the lower-energy section for the dBH type chain.

Note added. The scaling of the entanglement entropy and its quantum quench dynamics have been studied for the dBH model in the two accompanying papers [26, 33]. The results drawn from there are consistent with the spectral results presented in this work.

* Contact author.
chenjie666@xhu.edu.cn

† Contact author.
chunchen@sjtu.edu.cn

‡ Contact author.
xiaoqunwang@zju.edu.cn

- [1] A. Morningstar, L. Colmenarez, V. Khemani, D. J. Luitz, and D. A. Huse, Avalanches and many-body resonances in many-body localized systems, *Phys. Rev. B* **105**, 174205 (2022).
- [2] J. Šuntajs, J. Bonča, T. Prosen, and L. Vidmar, Quantum chaos challenges many-body localization, *Phys. Rev. E* **102**, 062144 (2020).
- [3] P. Sierant, M. Lewenstein, A. Scardicchio, L. Vidmar, and J. Zakrzewski, Many-Body Localization in the Age of Classical Computing, *arXiv:2403.07111* (2024).
- [4] M. Kiefer-Emmanouilidis, R. Unanyan, M. Fleischhauer, and J. Sirker, Evidence for Unbounded Growth of the Number Entropy in Many-Body Localized Phases, *Phys. Rev. Lett.* **124**, 243601 (2020).
- [5] J. Šuntajs, J. Bonča, T. Prosen, and L. Vidmar, Ergodicity breaking transition in finite disordered spin chains, *Phys. Rev. B* **102**, 064207 (2020).
- [6] D. M. Long, P. J. Crowley, V. Khemani, and A. Chandran, Phenomenology of the Prethermal Many-Body Localized Regime, *Phys. Rev. Lett.* **131**, 106301 (2023).
- [7] D. Aceituno Chávez, C. Artiago, T. Klein Kvorning, L. Herviou, and J. H. Bardarson, Ultraslow Growth of Number Entropy in an ℓ -Bit Model of Many-Body Localization, *Phys. Rev. Lett.* **133**, 126502 (2024).
- [8] D. J. Luitz, N. Laflorencie, and F. Alet, Many-body localization edge in the random-field Heisenberg chain, *Phys. Rev. B* **91**, 081103 (2015).
- [9] P. Sierant, M. Lewenstein, and J. Zakrzewski, Polynomially Filtered Exact Diagonalization Approach to Many-Body Localization, *Phys. Rev. Lett.* **125**, 156601 (2020).
- [10] J. Colbois, F. Alet, and N. Laflorencie, Interaction-Driven Instabilities in the Random-Field XXZ Chain, *Phys. Rev. Lett.* **133**, 116502 (2024).
- [11] M. Hopjan and F. Heidrich-Meisner, Many-body localization from a one-particle perspective in the disordered one-dimensional Bose-Hubbard model, *Phys. Rev. A* **101**, 063617 (2020).
- [12] T. Orell, A. A. Michailidis, M. Serbyn, and M. Silveri, Probing the many-body localization phase transition with superconducting circuits, *Phys. Rev. B* **100**, 134504 (2019).
- [13] P. Sierant and J. Zakrzewski, Many-body localization of bosons in optical lattices, *New J. Phys.* **20**, 043032 (2018).
- [14] R. Yao and J. Zakrzewski, Many-body localization in the Bose-Hubbard model: Evidence for mobility edge, *Phys. Rev. B* **102**, 014310 (2020).
- [15] A. Lukin, M. Rispoli, R. Schittko, M. E. Tai, A. M. Kaufman, S. Choi, V. Khemani, J. Léonard, and M. Greiner, Probing entanglement in a many-body-localized system, *Science* **364**, 256 (2019).
- [16] J. Léonard, S. Kim, M. Rispoli, A. Lukin, R. Schittko, J. Kwan, E. Demler, D. Sels, and M. Greiner, Probing the onset of quantum avalanches in a many-body localized system, *Nat. Phys.* **19**, 481 (2023).
- [17] C. Kollath, A. M. Läuchli, and E. Altman, Quench Dynamics and Nonequilibrium Phase Diagram of the Bose-Hubbard Model, *Phys. Rev. Lett.* **98**, 180601 (2007).
- [18] J. H. Van Vleck, On σ -Type Doubling and Electron Spin in the Spectra of Diatomic Molecules, *Phys. Rev.* **33**, 467 (1929).
- [19] C. Cohen-Tannoudji, J. Dupont-Roc, and G. Grynberg, *Atom-Photon Interactions* (John Wiley & Sons, 1998).
- [20] D. Herschbach, The Van Vleck transformation in perturbation theory, *MIT Lecture Notes* (1982).
- [21] M. A. Cazalilla, One-dimensional optical lattices and impenetrable bosons, *Phys. Rev. A* **67**, 053606 (2003).
- [22] S. Basak and H. Pu, Strongly interacting two-component coupled Bose gas in optical lattices, *Phys. Rev. A* **104**, 053326 (2021).
- [23] J. M. Zhang and R. X. Dong, Exact diagonalization: the Bose-Hubbard model as an example, *European Journal of Physics* **31**, 591 (2010).
- [24] V. Oganesyan and D. A. Huse, Localization of interacting fermions at high temperature, *Phys. Rev. B* **75**, 155111 (2007).
- [25] Y. Y. Atas, E. Bogomolny, O. Giraud, and G. Roux, Distribution of the Ratio of Consecutive Level Spacings in Random Matrix Ensembles, *Phys. Rev. Lett.* **110**, 084101 (2013).
- [26] J. Chen, C. Chen, and X. Wang, Eigenstate properties of the disordered Bose-Hubbard chain, *Front. Phys.* **19**, 43207 (2024).
- [27] M. Serbyn, Z. Papić, and D. A. Abanin, Local Conservation Laws and the Structure of the Many-Body Localized States, *Phys. Rev. Lett.* **111**, 127201 (2013).
- [28] D. A. Huse, R. Nandkishore, and V. Oganesyan, Phenomenology of fully many-body-localized systems, *Phys. Rev. B* **90**, 174202 (2014).
- [29] A. Chandran, I. H. Kim, G. Vidal, and D. A. Abanin, Constructing local integrals of motion in the many-body localized phase, *Phys. Rev. B* **91**, 085425 (2015).
- [30] S. D. Geraedts, R. N. Bhatt, and R. Nandkishore, Emergent local integrals of motion without a complete set of localized eigenstates, *Phys. Rev. B* **95**, 064204 (2017).
- [31] S. D. Huber and N. H. Lindner, Topological transitions for lattice bosons in a magnetic field, *Proc. Natl. Acad. Sci.* **108**, 19925 (2011).
- [32] C. Lacroix, P. Mendels, and F. Mila, *Introduction to frustrated magnetism: materials, experiments, theory*, Vol. 164, p. 537 (Springer Science & Business Media, 2011).
- [33] J. Chen, C. Chen, and X. Wang, Symmetry- and Energy-Resolved Entanglement Dynamics in Disordered Bose-Hubbard Model, *arXiv:2303.14825* (2023).